

## Effect of the Second-Generation Vascular Disrupting Agent OXi4503 on Tumor Vascularity

Howard W. Salmon and Dietmar W. Siemann

**Abstract Purpose:** As first-generation small-molecule vascular disrupting agents (VDA) have begun to enter clinical trials, second-generation agents are under active development. One such agent is the combretastatin A4 disodium phosphate (CA4P) analogue OXi4503 (CA1P).  
**Experimental Design:** C3H/HeJ mice bearing KHT sarcomas were treated with CA4P and OXi4503 and the effect on tumor vasculature was determined by evaluating the extent of vascular shutdown (Hoechst-33342 vessel staining) and tumor perfusion inhibition (dynamic contrast-enhanced magnetic resonance imaging). Dynamic contrast-enhanced magnetic resonance imaging and tumor necrosis end points also were used to examine the pathophysiologic tumor effects following repeated exposures to these agents.  
**Results:** Single doses of either agent (CA4P, 100 mg/kg; OXi4503, 25 mg/kg) resulted in an 80% to 90% reduction in tumor perfusion 4 hours after treatment. Whereas recovery in tumor perfusion was observed 48 hours posttreatment, this recovery was significantly slower in mice treated with OXi4503. Tumors re-treated with either VDA 72 hours after the first drug exposure showed a similar reduction and recovery in tumor perfusion. Histologic evidence showed the presence of a smaller viable rim after exposure to OXi4503 than that observed after CA4P treatment. Furthermore, the extent of recovery of tumor necrosis 72 hours after drug treatment was less for OXi4053.  
**Conclusions:** The present studies show that the second-generation VDA OXi4503 possesses significant antivasular effects in solid tumors. Importantly, the vasculature of tumors of mice that had received an initial dose this agent was as responsive to a subsequent treatment.

It has been well established that if a tumor is to grow to a clinically relevant size, it must induce a supporting vasculature (1, 2). It has also been shown that the rapid growth and development of the tumor places tremendous strains on this new vasculature, resulting in major vascular abnormalities (3, 4). These vascular abnormalities consist of temporary occlusions, a rapidly dividing endothelial population, blind ends, leaky vessels, and a reduction in pericytes (5, 6). Importantly, the successful treatment of the cancer by conventional therapies may be affected by these vascular abnormalities (3, 4).

In recent years, therapies targeted specifically at exploiting these tumor vasculature abnormalities have been under investigation (5–7). A class of vascular disrupting agents (VDA) that cause a rapid and selective shutdown of the tumor

vascular by damaging tumor vessel endothelium have now been identified (8). Treatment with such agents results in the arrest of the blood flow, which in turn acts to starve the tumor of the oxygen and nutrients it needs to survive (6, 9). The lead drug in this class of agents is the tubulin binding agent combretastatin A4 disodium phosphate (CA4P; refs. 5, 9, 10). This agent has been extensively examined in various preclinical and clinical trials with encouraging results (11, 12).

Tubulin binding agents like CA4P disorganize the microtubules within endothelial cells; specifically, they bind to the  $\beta$ -tubulin subunits, preventing the formation of microtubules (9, 13). After treatment with CA4P, newly formed daughter endothelial cells have been observed to undergo shape changes (14, 15) as a consequence of cytoskeletal alterations. These shape changes are thought to lead to the increase in vascular permeability observed after treatment with CA4P (15). Finally, these endothelial cells detach, the vascular wall collapses, and tumor cell death occurs as a consequence of tumor blood flow obstructions (6, 9).

Because the periphery of the tumor is mainly fed through the surrounding vessels of normal tissues, a "viable rim" of tumor cells is seen to remain after treatment with these agents. As a result, VDAs alone are unlikely to be a curative (9). Consequently, there has been considerable interest in evaluating the antitumor effects of these agents when they are combined with traditional anticancer therapies (5, 9). For the case of CA4P, results have shown that the VDA could enhance the

**Authors' Affiliation:** Department of Radiation Oncology, Shands Cancer Center, University of Florida, Gainesville, Florida

Received 1/23/06; revised 3/31/06; accepted 4/27/06.

**Grant support:** U.S. Public Health Service grant CA-84408.

The costs of publication of this article were defrayed in part by the payment of page charges. This article must therefore be hereby marked *advertisement* in accordance with 18 U.S.C. Section 1734 solely to indicate this fact.

**Requests for reprints:** Howard W. Salmon, Department of Radiation Oncology, University of Florida, Box 100385, 2000 Southwest Archer Road, Gainesville, FL 32610. Phone: 352-392-0655; E-mail: hwsalmon@ufl.edu.

©2006 American Association for Cancer Research.

doi:10.1158/1078-0432.CCR-06-0163

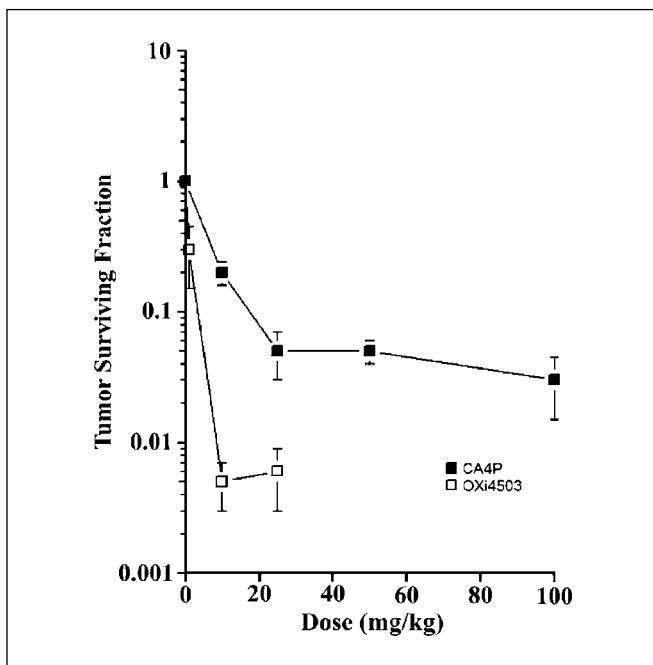


Fig. 1. Clonogenic cell survival in KHT sarcomas of mice treated with a range of doses of CA4P and OXi4503. Points, mean of three to five tumors; bars, SE.

effects of radiation (16–18), hyperthermia (19), chemotherapy (10, 20–23), and radioimmunotherapy (24, 25).

The entrance of CA4P into clinical trials (9, 11, 12) has also spurred the development of second-generation VDAs. The present study examined the efficacy of one such agent (OXi4503) by comparing its antivasular effects with those of CA4P in the KHT sarcoma model.

## Materials and Methods

**Animal and tumor model.** All research works were governed by the principles of the Guide for the Care and Use of Laboratory Animals and approved by the University of Florida Institutional Animal Care and Use Committee. Female C3H mice, ages 6 to 8 weeks, were obtained from The Jackson Laboratory (Bar Harbor, ME). KHT sarcoma cells (17) were injected ( $2 \times 10^5$ ) into a single hind limb of the mice.

**Drug treatment.** For all experiments, mice were randomly allocated to various experimental groups. Both CA4P and OXi4503 (OXiGENE, Waltham, MA) were prepared in saline and injected i.p. (0.01 mL/g body weight). Tumor-bearing mice were treated with either CA4P at 100 mg/kg or OXi4503 at 25 mg/kg.

**Clonogenic cell survival.** Tumor-bearing mice were killed 24 hours after treatment and their tumors removed and dissociated. The cells were then counted and incubated at various dilutions in 60-mm dishes. After 2 weeks of incubation at 37°C, colonies of  $\geq 50$  cells were counted. Ten days later, the number of colonies in each of the groups was counted and cell survival was determined.

**Vascular shutdown studies.** Hoechst-33342 (Sigma) solution was administered at 40 mg/kg i.v. at various times after CA4P/OXi4503 treatment. One minute after Hoechst-33342 injection, the mice were killed, the tumors excised, and 10- $\mu$ m cryostat sections were prepared. Vessel counts were done using a Chalkley point array for random sample analysis (26). For each tumor, the mean vessel density was determined based on a minimum of six sections per tumor. Statistical analysis was based on a mean of three to five tumors per group ( $\pm$ SE).

**Tumor perfusion measurement.** Tumor perfusion was determined in KHT tumor-bearing mice using the magnetic resonance imaging (MRI) contrast agent gadolinium-diethylenetriaminepentaacetic acid (GdDTPA) "Omniscan (gadodiamide)." Contrast-enhanced MRI measurements were made before and at 4-, 24-, and 48-hour time intervals after a single-dose treatment or 4, 24, 72, 96, and 144 hours after repeat dosing treatments. Image sets were acquired using an 11-T magnet (Oxford Instruments, horizontal bore of 40-cm diameter). The mice were anesthetized with 2% isoflurane via induction chamber and maintained with 1.25% isoflurane via face mask (reducing isoflurane concentration by 0.25% for every 20 minutes). A flow of warmed air was used to maintain the body temperature of the animals while in the magnet.

Contrast enhancement measurements were made using a  $T_1$ -weighted spin-echo sequence (TE, 12 ms; TR, 130 ms; field of view,  $20 \times 20$  mm; 128 phase-encode increments and 256 data points, zero-filled to  $256 \times 256$ ; slice thickness, 1 mm). For all animals, one 14-slice data set was acquired before the introduction of GdDTPA (0.2 mmol/kg) via bolus tail-vein injection. Subsequent data sets were collected from all 14 slices throughout the tumor for a period of 15 minutes postinjection to monitor inflow of GdDTPA into the tumor. Maps of the initial rate of inflow of GdDTPA into the tumors were generated by subtracting the image acquired before GdDTPA was introduced from the five images acquired 3, 6, 9, 12, and 15 minutes later. The resultant contrast-enhanced tumor images were assessed quantitatively by plotting the mean signal intensity in a region of interest defined within the tumor (excluding skin) against time after injection of contrast agent. Perfusion was then determined by measuring the integrating area under the signal intensity-time curve.

**Necrotic fraction assessment.** KHT tumor-bearing mice were treated with either CA4P (100 mg/kg) or OXi4503 (25 mg/kg), or kept as untreated controls. At 24, 72, 96, and 144 hours after treatment, three mice from each group were killed and tumors were removed and fixed in formalin for 24 hours before sectioning. Paraffin sections were taken from the center of each tumor and stained using H&E. After H&E staining, the sections were imaged under a morphometric microscope at  $\times 5$  magnification using the tile field mapping technique. The necrotic fraction was then determined for these sections using the NIH imaging software ImageJ. For each tumor, the mean necrotic fraction was determined based on a minimum of three sections per tumor. Statistical analysis was based on a mean of three to five tumors per group ( $\pm$ SE).

**Statistical analysis.** Results were analyzed using ANOVA in combination with Scheffé's post hoc procedure. In all cases, differences were considered statistically significant at  $P < 0.05$ .

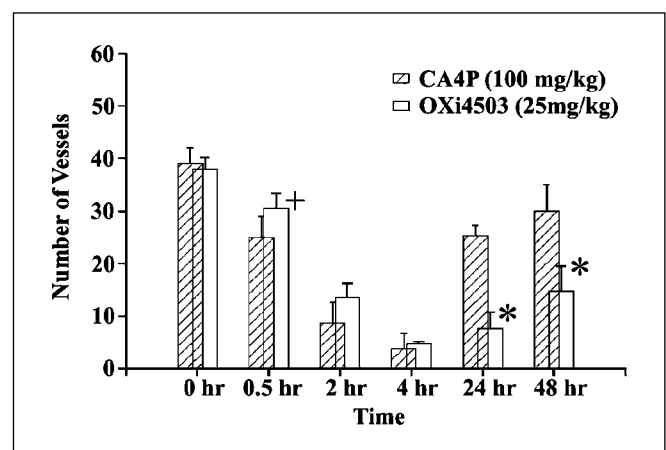


Fig. 2. Effect of VDA treatment on patent tumor blood vessels. Tumor-bearing mice were treated with a single dose of either CA4P (100 mg/kg) or OXi4503 (25 mg/kg). At various times after treatment, the number of vessels actively involved in blood flow was determined (Materials and Methods). Columns, mean of three to five tumors; bars, SE. \*,  $P < 0.05$ , statistically significant from the pretreatment values; \*,  $P < 0.05$ , statistically significant from the CA4P group.

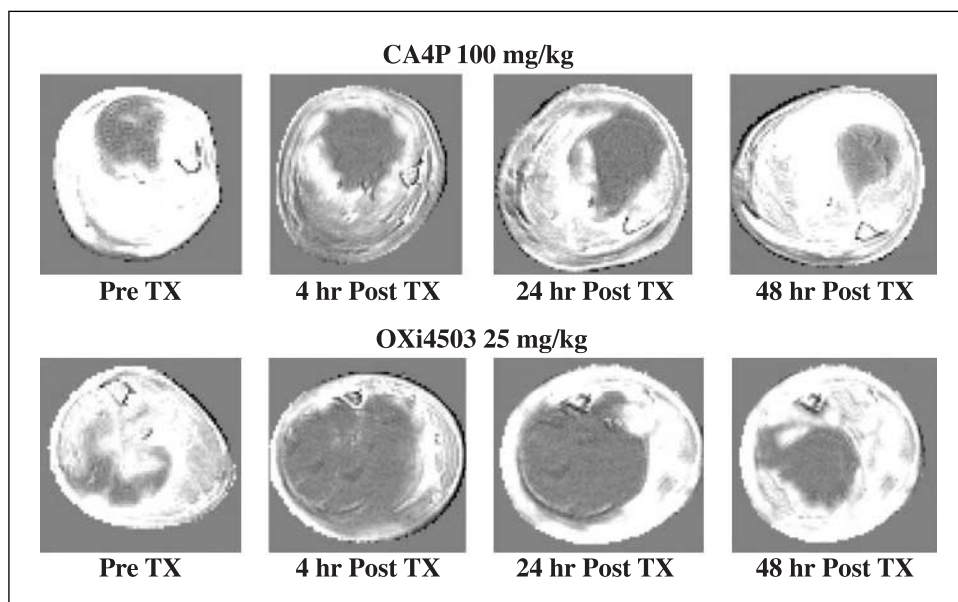


Fig. 3. Tumor perfusion images at various times before and after VDA treatment (CA4P, 100 mg/kg; OXi4503, 25 mg/kg). Before and after measurements were made on the same mouse. White, perfused tissue.

## Results

The present study aimed to compare the antivasular activity of the VDA CA4P with its second-generation analogue OXi4503 in the KHT rodent sarcoma grown in C3H mice. The disruption of the tumor vasculature leads to secondary tumor cell death due to ischemia (9). To quantify this effect, clonogenic cell survival studies were done. The results shown in Fig. 1 indicate that for both agents investigated, tumor cell survival initially decreases as the VDA treatment dose increases and then plateaus. On the basis of these results and in keeping with previous preclinical investigations using these agents (27–30), doses of 100 and 25 mg/kg of CA4P and OXi4503, respectively, were chosen for subsequent pathophysiological evaluations.

The antivasular effects of these agents were established by counting the number of perfused tumor blood vessels as function of time after drug exposure (Fig. 2). These results showed that within 30 minutes of treatment with either CA4P or OXi4503, a significant reduction in perfused vessels was apparent. For both agents, an 80% to 90% reduction in perfused vessels was seen 4 hours after treatment. By 24 hours after drug exposure, some vascular recovery occurred but this recovery was found to be significantly slower in the tumors of OXi4503-treated mice.

Changes in tumor perfusion following treatment with single doses of CA4P or OXi4503 were also determined using dynamic contrast-enhanced MRI (Fig. 3). GdDTPA-enhanced images taken before treatment showed that whereas some tumors had poorly perfused centers before treatment, in all cases GdDTPA enhancement was impaired after treatment with either CA4P or OXi4503. These images were quantified (Fig. 4) and the results showed that GdDTPA inflow into KHT tumors was significantly reduced 4 hours after treatment. At later time points, tumor perfusion started to recover (Fig. 4); however, as was also seen in the Hoechst 33342 staining study (Fig. 2), the rate of this recovery was significantly slower in the OXi4503 treatment group. By 48 hours, tumor perfusion continued to improve, leading to values that were 75% and 63% of those found in control tumors for CA4P- and OXi4503-treated mice.

To evaluate the effect of repeat VDA dosing on tumor perfusion, KHT tumor-bearing mice were treated with two doses of either CA4P or OXi4503 separated by 72 hours. MRI-based perfusion measurements were made 4, 24, 48, and 72 hours after each of the two VDA doses. The results over the initial 0 to 48 hour time period (Fig. 5) showed perfusion patterns similar to those seen in the single dose study (Fig. 4). However, by 72 hours after treatment, tumor perfusion in the CA4P-treated animals had returned to pretreatment values. In contrast, the OXi4503-treated mice tumor perfusion recovered at a significantly slower rate, with median tumor perfusion at 72 hours being 62% of pretreatment values. At this time, all animals were re-treated and the vascular response to the second dose of the VDA was determined 4, 24, and 72 hours later. The results showed that by 4 hours after the second treatment, tumor perfusion was once again dramatically reduced for both agents (Fig. 5). Although the median tumor perfusion in the OXi4503-treated group seemed to be lower than that achieved with CA4P treatment, the difference was not significant. At later

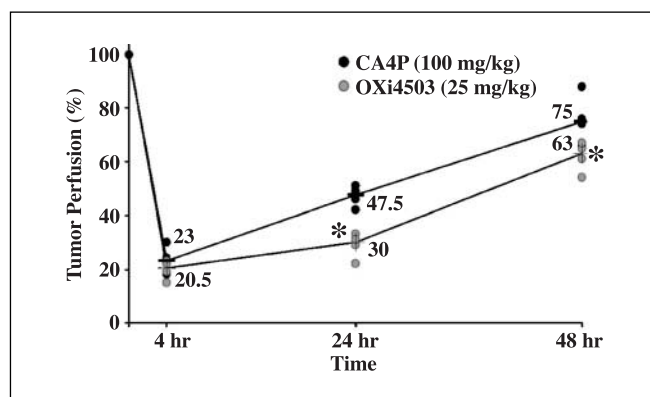


Fig. 4. Tumor perfusion after treatment with a single dose of CA4P (100 mg/kg) or OXi4503 (25 mg/kg). Dynamic contrast-enhanced MRI perfusion measurements were made on individual mice, each being assessed at every time point. Points, median group response as a function of time after treatment. \*,  $P < 0.05$ , statistically significant from CA4P group.

times, perfusion recovered in all tumors in a manner similar to that seen after the initial treatment.

Histology assessment done on the tumors of mice treated with two doses of the VDAs separated by 72 hours indicated that, 24 hours following treatment with either VDA, the percent tumor necrosis rose to ~80% to 90% (Fig. 6). At later times, tumor necrosis recovered in a manner similar to that seen in the dynamic contrast-enhanced MRI study, with a somewhat slower rate of recovery observed in the tumors of mice treated with OXi4503 (Fig. 6). In addition, as was the case for the dynamic contrast-enhanced MRI perfusion measurements, the effect of the second VDA treatment on tumor necrosis and its subsequent recovery was similar to that seen following the first treatment dose.

## Discussion

In the early eighties, studies carried out by Denekamp and colleagues showed that endothelial proliferation was considerably higher in tumors regardless of their size, and suggested that this high proliferation rate might prove to be a useful target in the treatment of cancer (31, 32). In an effort to exploit this possibility, a number of agents that target tumor blood vessels have now been identified and the lead candidates have entered clinical trials (5, 9, 12). Hallmark characteristics of such VDAs are reduction in tumor blood flow, induction of widespread tumor necrosis, secondary tumor cell death due to ischemia, and the presence of a surviving rim of neoplastic cells at the tumor periphery (6, 9). This "viable rim" is thought to result from the tumor cells in this area receiving oxygen and nutrients from the surrounding normal tissue vasculature. Consequently, it is generally believed that such agents will have their greatest utility when used in conjunction with conventional anticancer therapies (5, 6, 9).

Clinically, dynamic contrast-enhanced MRI, a method that assesses changes in tumor blood perfusion through the use of a gadolinium-based contrast agent, has emerged as an important tool in determining the antivasular effects of VDA treatment (33). In the present study, this technique was compared with the established preclinical indicators of VDA treatment efficacy

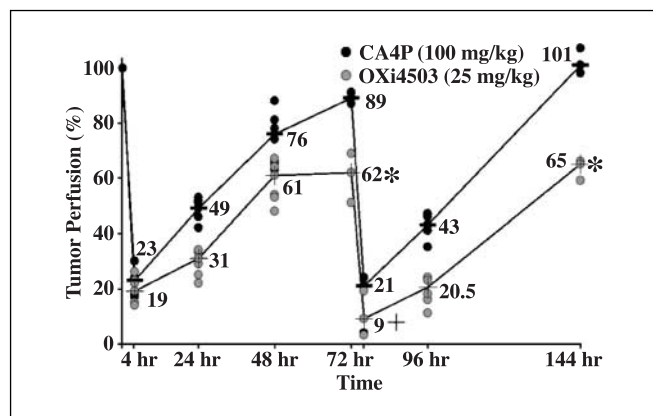


**Fig. 5.** Tumor perfusion after treatment with two doses of VDAs CA4P (100 mg/kg) and OXi4503 (25 mg/kg). The first dose was administered at time 0; the second was given 72 hours later. Changes in tumor perfusion of individual mice as a function of time after treatments; points, median. \*,  $P < 0.05$ , statistically significant from CA4P group; +, not statistically significant from CA4P (76 hours) or from both agents at the 4-hour time point.

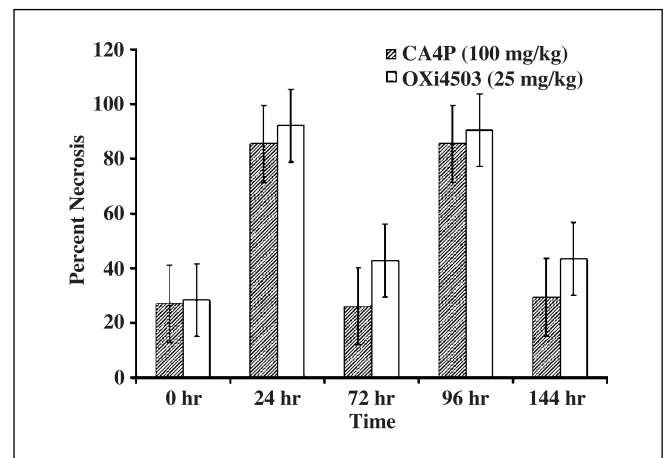


**Fig. 6.** Necrotic fraction measurements in KHT tumors following repeated doses of either CA4P (100 mg/kg) or OXi4503 (25 mg/kg). Doses were given 72 hours apart. Columns, mean change in tumor necrotic fraction as a function of time; bars, SE.

(i.e., vessel density and tumor necrosis). In addition, the efficacies of single and repeat exposures to VDAs CA4P and OXi4503 were assessed and compared in the KHT sarcoma tumor model.

Initial investigations into the antivasular properties of these agents revealed that tumors treated with these agents suffered a rapid loss of patent blood vessels (Fig. 2). For both agents, a similar nadir in vessel number was reached 4 hours after treatment but the effect of OXi4503 treatment on the tumor vasculature clearly lasted longer than that observed following CA4P exposure. When these antivasular effects were assessed using dynamic contrast-enhanced MRI (Figs. 3 and 4), similar results were seen. Both agents led to comparable reductions in tumor perfusion 4 hours after treatment, and once again, vascular recovery (as measured by tumor perfusion) was found to be significantly slower in tumors of mice treated with OXi4503.

Because in the clinic patients receive more than a single dose of a given VDA, it was of interest to examine the effect on tumor vasculature of administering a VDA to a tumor-bearing host that had undergone a prior treatment. Specifically, the efficacy of delivering a second dose of either CA4P or OXi4503 72 hours after the first was examined. The results (Fig. 5) showed that for both agents the effect of the second dose mostly mirrored that of the first. Indeed, once again the results suggest a greater antivasular efficacy of OXi4503 as compared with CA4P.

An established method for determining VDA treatment efficacy in preclinical investigations has been the measurement of the extent of tumor necrosis. Such measurements are not easily made in patients undergoing VDA therapy. This being the case, it seemed appropriate to compare the dynamic contrast-enhanced MRI assessments (which can be made in the clinic) to this established preclinical response end point. To achieve this, necrosis measurements were made in KHT sarcoma-bearing mice undergoing the repeat dosing regimen. The results (Fig. 6) showed a pattern of fluctuating necrotic fraction consistent with the perfusion changes measured by dynamic contrast-enhanced MRI. Once again, in the OXi4503 treatment group, a longer-lasting effect on tumor necrosis was seen, a result consistent with both the vessel density and dynamic contrast-enhanced



MRI data. Further, the indication of more extensive necrosis following OXi4503 treatment is consistent with the observation of significantly greater cell kill (Fig. 1) and the presence of a smaller viable rim in this tumor model (29). Taken together, these data support the notion that OXi4503 may have some therapeutic advantages over CA4P (27, 29).

In summary, the association between VDA treatment-induced tumor necrosis and dynamic contrast-enhanced MRI-based perfusion measurements supports the continued use of the latter technique for the monitoring of patients receiving VDA therapy. Because MRI facilities are readily available in many hospitals, the clinical assessment of these

novel agents should therefore be readily feasible. The data presented in this study also indicate that tumors previously treated with a VDA will be susceptible to repeat treatments with such agents. Finally, the present studies provide additional preclinical evidence that the second-generation VDA OXi4503 holds significant promise and warrants further investigation.

## Acknowledgments

We thank the Evelyn F. & William L. McKnight Brain Institute of the University of Florida (Gainesville, FL) for the use of their Advanced Magnetic Resonance Imaging and Spectroscopy Facility and Optical Microscopy Facilities.

## References

- Denekamp J, Hill SA, Hobson B. Vascular occlusion and tumour cell death. *Eur J Cancer Clin Oncol* 1983; 19:271–5.
- Folkman J. Tumor angiogenesis: role in regulation of tumor growth. *Symp Soc Dev Biol* 1974;30:43–52.
- Harris AL. Hypoxia—a key regulatory factor in tumour growth. *Nat Rev Cancer* 2002;2:38–47.
- Vaupel P, Kallinowski F, Okunieff P. Blood flow, oxygen and nutrient supply, and metabolic microenvironment of human tumors: a review. *Cancer Res* 1989; 49:6449–65.
- Thorpe PE. Vascular targeting agents as cancer therapeutics. *Clin Cancer Res* 2004;10:415–27.
- Tozer GM, Kanthou C, Baguley BC. Disrupting tumour blood vessels. *Nat Rev Cancer* 2005;5:423–35.
- Denekamp J. Vascular attack as a therapeutic strategy for cancer. *Cancer Metastasis Rev* 1990;9:267–82.
- Chaplin DJ, Pettit GR, Parkins CS, Hill SA. Antivascular approaches to solid tumour therapy: evaluation of tubulin binding agents. *Br J Cancer Suppl* 1996;27: S86–8.
- Siemann DW, Chaplin DJ, Horsman MR. Vascular-targeting therapies for treatment of malignant disease. *Cancer* 2004;100:2491–9.
- Chaplin DJ, Pettit GR, Hill SA. Anti-vascular approaches to solid tumour therapy: evaluation of combretastatin A4 phosphate. *Anticancer Res* 1999; 19:189–95.
- Bilenker JH, Flaherty KT, Rosen M, et al. Phase I trial of combretastatin a-4 phosphate with carboplatin. *Clin Cancer Res* 2005;11:1527–33.
- Young SL, Chaplin DJ. Combretastatin A4 phosphate: background and current clinical status. *Expert Opin Investig Drugs* 2004;13:1171–82.
- Grosios K, Holwell SE, McGown AT, Pettit GR, Bibby MC. *In vivo* and *in vitro* evaluation of combretastatin A-4 and its sodium phosphate prodrug. *Br J Cancer* 1999;81:1318–27.
- Galbraith SM, Chaplin DJ, Lee F, et al. Effects of combretastatin A4 phosphate on endothelial cell morphology *in vitro* and relationship to tumour vascular targeting activity *in vivo*. *Anticancer Res* 2001;21: 93–102.
- Kanthou C, Tozer GM. The tumor vascular targeting agent combretastatin A-4-phosphate induces reorganization of the actin cytoskeleton and early membrane blebbing in human endothelial cells. *Blood* 2002;99: 2060–9.
- Landuyt W, Ahmed B, Nuyts S, et al. *In vivo* antitumor effect of vascular targeting combined with either ionizing radiation or anti-angiogenesis treatment. *Int J Radiat Oncol Biol Phys* 2001;49:443–50.
- Li L, Rojani A, Siemann DW. Targeting the tumor vasculature with combretastatin A-4 disodium phosphate: effects on radiation therapy. *Int J Radiat Oncol Biol Phys* 1998;42:899–903.
- Murata R, Siemann DW, Overgaard J, Horsman MR. Interaction between combretastatin A-4 disodium phosphate and radiation in murine tumors. *Radiother Oncol* 2001;60:155–61.
- Murata R, Overgaard J, Horsman MR. Combretastatin A-4 disodium phosphate: a vascular targeting agent that improves that improves the anti-tumor effects of hyperthermia, radiation, and mild thermoradiotherapy. *Int J Radiat Oncol Biol Phys* 2001;51: 1018–24.
- Grosios K, Loadman PM, Swaine DJ, Pettit GR, Bibby MC. Combination chemotherapy with combretastatin A-4 phosphate and 5-fluorouracil in an experimental murine colon adenocarcinoma. *Anticancer Res* 2000;20:229–33.
- Horsman MR, Murata R, Bredahl T, et al. Combretastatin novel vascular targeting drugs for improving anti-cancer therapy. *Combretastatin and conventional therapy. Adv Exp Med Biol* 2000;476: 311–23.
- Nelkin BD, Ball DW. Combretastatin A-4 and doxorubicin combination treatment is effective in a preclinical model of human medullary thyroid carcinoma. *Oncol Rep* 2001;8:157–60.
- Siemann DW, Mercer E, Lepler S, Rojani AM. Vascular targeting agents enhance chemotherapeutic agent activities in solid tumor therapy. *Int J Cancer* 2002;99:1–6.
- Pedley RB, Hill SA, Boxer GM, et al. Eradication of colorectal xenografts by combined radioimmunotherapy and combretastatin a-4 3-O-phosphate. *Cancer Res* 2001;61:4716–22.
- Pedley RB, El Emir E, Flynn AA, et al. Synergy between vascular targeting agents and antibody-directed therapy. *Int J Radiat Oncol Biol Phys* 2002; 54:1524–31.
- Hansen S, Grabau DA, Sorensen FB, Bak M, Vach W, Rose C. The prognostic value of angiogenesis by Chalkley counting in a confirmatory study design on 836 breast cancer patients. *Clin Cancer Res* 2000;6: 139–46.
- Hill SA, Toze GM, Pettit GR, Chaplin DJ. Preclinical evaluation of the antitumor activity of the novel vascular targeting agent Oxi 4503. *Anticancer Res* 2002; 22:1453–8.
- Hua J, Sheng Y, Pinney KG, et al. Oxi4503, a novel vascular targeting agent: effects on blood flow and antitumor activity in comparison to combretastatin A-4 phosphate. *Anticancer Res* 2003;23:1433–40.
- Rojani AM, Rojani MV. Morphologic manifestations of vascular-disrupting agents in preclinical models. London: Wiley; 2006. p. 81–94.
- Shi W, Horsman MR, Siemann DW. Combined modality approaches using vasculature-disrupting agents. *Vascular-targeted therapies in oncology*. London: Wiley; 2006. p. 123–36.
- Denekamp J, Hobson B. Endothelial-cell proliferation in experimental tumours. *Br J Cancer* 1982;46: 711–20.
- Denekamp J. Vascular endothelium as the vulnerable element in tumours. *Acta Radiol Oncol* 1984; 23:217–25.
- Galbraith SM, Maxwell RJ, Lodge MA, et al. Combretastatin A4 phosphate has tumor antivascular activity in rat and man as demonstrated by dynamic magnetic resonance imaging. *J Clin Oncol* 2003;21: 2831–42.